



Forces acting on a particle in a concentration gradient under an externally applied oscillating electric field

Yuan Luo and Levent Yobas

Citation: [Applied Physics Letters](#) **105**, 094105 (2014); doi: 10.1063/1.4894731

View online: <http://dx.doi.org/10.1063/1.4894731>

View Table of Contents: <http://scitation.aip.org/content/aip/journal/apl/105/9?ver=pdfcov>

Published by the [AIP Publishing](#)

Articles you may be interested in

[Role of solution conductivity in reaction induced charge auto-electrophoresis](#)

Phys. Fluids **26**, 042001 (2014); 10.1063/1.4869328

[Deformation, breakup and motion of a perfect dielectric drop in a quadrupole electric field](#)

Phys. Fluids **24**, 032105 (2012); 10.1063/1.3691655

[Measurements of the near-wall hindered diffusion of colloidal particles in the presence of an electric field](#)

Appl. Phys. Lett. **99**, 124104 (2011); 10.1063/1.3643136

[Mixing enhancement in microfluidic channel with a constriction under periodic electro-osmotic flow](#)

Biomechanics **4**, 014101 (2010); 10.1063/1.3279790

[Five-cross microfluidic network design free of coupling between electrophoretic motion and electro-osmotic flow](#)

Appl. Phys. Lett. **89**, 084101 (2006); 10.1063/1.2338570



Free online magazine

MULTIPHYSICS SIMULATION

[READ NOW ▶](#)

COMSOL

Forces acting on a particle in a concentration gradient under an externally applied oscillating electric field

Yuan Luo and Levent Yobas^{a)}

Department of Electronic and Computer Engineering, Hong Kong University of Science and Technology, Hong Kong, People's Republic of China

(Received 29 May 2014; accepted 24 August 2014; published online 5 September 2014)

We report a force field on a particle in a concentration (conductivity) gradient under an externally applied oscillating electric field. The conductivity gradient was established through integrated microcapillaries bridging high- and low-conductivity streams in dedicated microchannels. Particles in low-conductivity electrolyte were observed to experience a strong force with the application of an oscillating field and pulled to the microcapillary openings where they were held against the flow. Particle trapping was accompanied by a concurrent electrolyte injection from high- to low-conductivity channel, triggered with the externally applied field and further contributed to the conductivity gradient near the trapping sites. We experimentally evaluated the force dependence on the magnitude and frequency of the excitation field for 10 μm polystyrene particles immersed at various conductivity levels. The experiments suggest that the observed force cannot be simply explained by dielectrophoresis or diffusiophoresis alone and further requires the consideration of a so-called concentration polarization force. This force has been rather recently postulated based on a theoretical treatment and yet to be experimentally validated. Using the theoretical treatment of this force, together with fluidic drag and diffusiophoresis, we correctly predicted trapping trajectories of particles based on a simultaneous solution of Poisson-Nernst-Planck and Stokes equations. The predicted and measured trapping velocities were found in reasonable agreement (within a factor of <1.6), suggesting that the consideration of the concentration polarization force is necessary for describing the observed particle behavior. © 2014 AIP Publishing LLC.

[<http://dx.doi.org/10.1063/1.4894731>]

With the advancement of the field of microfluidics, electrokinetic forces have gained tremendous attention not only for their appealing properties in dynamic control of particles and fluids but also their rich physical behavior calling for a deeper understanding.¹ Techniques, wherein such forces arise, namely, electroosmosis,² electrophoresis (EP),³ electrowetting,⁴ and dielectrophoresis (DEP),⁵ have become mainstream whereas those that are relatively new additions to the field including the induced charge electrokinetic,⁶ and diffusiophoresis (DP)⁷ are somewhat less explored.

Nearly a decade ago, Kang and Li⁸ predicted the existence of a new type of electrokinetic force that is likely to be exerted on a particle in an electrolyte solution with a conductivity (concentration) gradient under an applied electric field. The concentration-polarization force (the CP force), as coined by the authors, is distinct from those arising from local variations in dielectric properties of the fluid due to Joule heating and believed to originate from two mechanisms, both caused by the concentration gradient. One involves electrohydrodynamic (EHD) pressure gradient across the particle as a result of the induced “free” charges while the other engages dielectric force due to the induced nonuniform electric field. The authors performed a detailed theoretical analysis involving the perturbation of electric, concentration, and hydrodynamic fields, as well as the integration of Maxwell and hydrodynamic stress tensors. They

concluded that such force should be of a comparable magnitude to electrophoretic forces while an order of magnitude greater than those encountered in DEP. The CP force, excluding few studies alluding to its existence,^{9,10} has been rarely explored and remains to be experimentally validated.

This letter presents an experimental account of a force field in a microfluidic device that is likely to be the candidate for the CP force. The device has been initially built for trapping individual cells or particles at a microcapillary opening under the influence of DEP.¹¹ In the device, a pair of integrated short microcapillaries is utilized to deliver an oscillating electric field to a stream of cells or particles which is at a lower conductivity than the streams of electrolyte injected on the opposite ends of the microcapillaries and to which a voltage oscillation is externally applied using wire electrodes [Fig. 1(a)]. The microcapillaries are designed to squeeze field lines and distort the spatial distribution of the field into a nonuniform profile in order to induce DEP. Although cells and dielectric particles are shown to be effectively trapped at the microcapillary openings, Fig. 1(b), the latter strikingly occurs at a field frequency range where they should be repelled in accordance with negative DEP (nDEP) since the particles get less polarized than the immersion medium. Indeed, replacing the electrolyte with eutectic gallium-indium (EGaIn, Sigma-Aldrich), a liquid metal, unravels the nDEP response, and the particles start to get repelled by the microcapillary openings within the same frequency range, Fig. 1(c). This suggested that, with the applied voltage delivered through liquid electrolyte in the device, a force other

^{a)}Author to whom correspondence should be addressed. Electronic mail: eelyobas@ust.hk

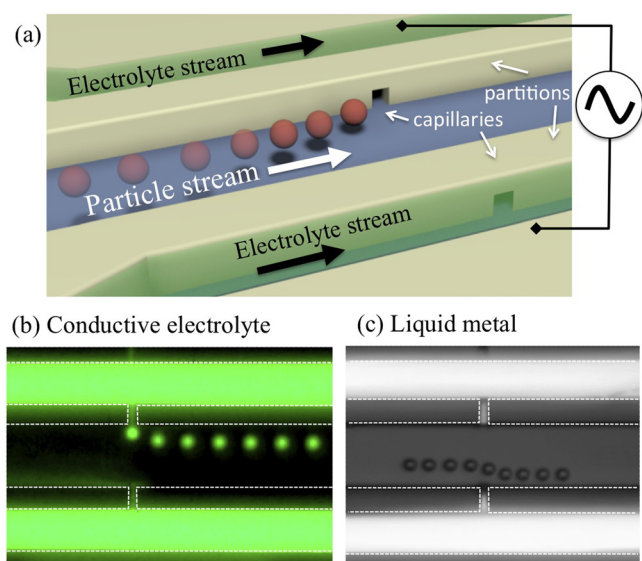


FIG. 1. (a) 3D rendering of the microdevice. A pair of integrated microcapillaries in face-to-face alignment is utilized to bridge two outer electrolyte channels and a center particle channel. (b) and (c) Overlays of high-speed video microscopy stills taken at a rate of 4000 fps reveal the trajectories of 10 μm carboxyl-modified polystyrene particles moving under a pressure-driven flow at a rate of 0.17 $\mu\text{l}/\text{min}$ (from right to left). The lateral deviations along the trajectories are in response to an externally applied voltage oscillation at 500 kHz. The two outer channels contained either (b) a fluorescein-dyed electrolyte phosphate buffered saline (PBS) solution at a conductivity of 15 mS/cm or (c) liquid metal (EGaN). The electrolyte streams were injected at a rate of 0.68 $\mu\text{l}/\text{min}$ under pressure-driven flow (from right to left). The particles were suspended in dilute PBS at a conductivity of 100 $\mu\text{S}/\text{cm}$. The microcapillaries were at a nominal width and depth of 6 μm . The dashed lines outline the channel and microcapillary boundaries. The voltage magnitude: (b) 141 and (c) 18 V-rms.

than that caused by conventional DEP is at play. The nature of such force has been investigated here by measuring the dependence of the particle velocity on the applied voltage rms magnitude and frequency in relation to the conductivity (concentration) set values of the immersion medium for a fixed particle size. Experimental measurements and numerical simulations have been compared and found in convincing agreement in support of our hypothesis.

The microdevices were fabricated in polydimethylsiloxane (PDMS) through soft-lithography process as previously described.¹¹ Briefly, microfluidic channels including the two outer channels (30 μm wide) and the center channel (50 μm wide) were moulded out of a photoresist film (SU-8, Microchem, MA) that was patterned at a thickness of 4–5 μm on a microstructured silicon wafer. The channels are separated by a pair of PDMS partitions (20 μm wide) with microcapillaries replicated from silicon ridge structures that were defined as either 2 or 6 μm wide and deep by a prior step of deep reactive ion etch (DRIE). PDMS (Sylgard 184, Dow Corning) with a base material and curing agent mixed at 10:1 w/w was degassed and cured over the template for half an hour at 120 $^{\circ}\text{C}$. The cured PDMS slab was punched with inlet/outlet holes and then bonded onto a glass slide to cover the channels immediately upon oxygen-plasma surface activation (for 40 s at 40 W). The two outer channels were injected with phosphate buffered saline (PBS, 15 mS/cm, pH 7.4) as the electrolyte while the center channel was delivered with PBS diluted to the desired conductivity level using

deionized water. Carboxyl-modified polystyrene microspheres (5 and 10 μm , Bangs Laboratories) were suspended in the latter whereas fluorescein was dissolved in the electrolyte for staining. The conductivity and pH readings were taken by using a meter (SevenGo Pro, Mettler-Toledo). Flow rates were controlled via dedicated syringe pumps (Harvard Apparatus). Copper wires were placed in the reservoirs of the outer channels and connected to a waveform generator (AV-151B-C, Avtech, Canada). The applied voltage was monitored through an oscilloscope (2205GN, Tektronics, OR). An epifluorescence microscope (FN1; Nikon, Japan) equipped with a mercury lamp (100 W) and a high-speed camera (Phantom, Vision Research, NJ) was used to capture and transfer images to a computer for the subsequent analysis.

Fig. 2 presents trajectories of 5 and 10 μm dielectric particles in superimposed stills from time-lapse videos revealing their lateral deviations in response to an externally applied voltage oscillation at 141 V-rms 500 kHz (the flow direction from right to left). As can be seen, lateral deviations in particle trajectories, i.e., whether particles be trapped or repelled by a microcapillary opening, mainly depend on the particle size and the conductivity of the immersion medium. At a low immersion conductivity of 10 $\mu\text{S}/\text{cm}$, particles of either size were found to be trapped and held against the microcapillary opening as long as the applied voltage was maintained, Fig. 2(a). Note that, in these immersion conductivity values, the particles were repelled throughout the range from 0.5 to 500 kHz when the microcapillaries were filled with liquid metal instead. An increase in the immersion

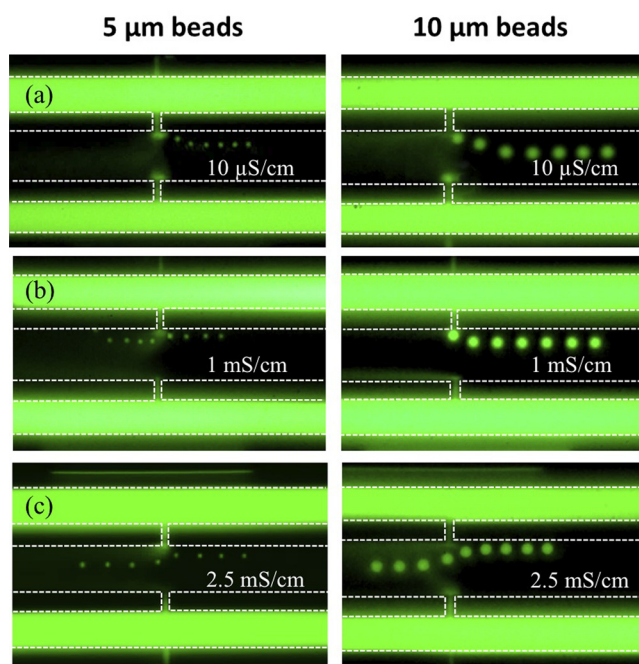


FIG. 2. Dependence of particle trajectory on the particle size (5 and 10 μm) and the immersion conductivity level at (a) 10 $\mu\text{S}/\text{cm}$, (b) 1, and (c) 2.5 mS/cm in response to an externally applied voltage (141 V-rms, 500 kHz). The conductivity of the electrolyte in the outer channels was 15 mS/cm. The electrolyte streams were maintained at a rate of 0.68 $\mu\text{l}/\text{min}$ while the particle stream was injected at 0.17 $\mu\text{l}/\text{min}$ under pressure-driven flow (from right to left). Overlays of high-speed video microscopy stills were taken at a rate of 4000 fps. The microcapillaries were at a nominal width and depth of 6 μm . The dashed lines outline the channel and microcapillary boundaries.

conductivity by two orders of magnitude (up to 1 mS/cm) did not cause a noticeable change in the trajectories of 10 μm particles; however, it did so in the trajectories of 5 μm particles, as the latter could no longer be trapped and were rather found repelled by the microcapillary opening, Fig. 2(b). With a further increase in the immersion conductivity up to 2.5 mS/cm, 10 μm particles were also observed to be repelled and could no longer be trapped, Fig. 2(c). Since the electrolyte was stained, it became evident that the particles that appeared to be repelled, in fact, followed the streamlines as a natural outcome of laminar flow rather than being subjugated to a repulsive force of dielectric nature. As shown, the electrolyte streams, with the applied voltage, overcome the hydraulic resistance of the microcapillaries, and began to displace the particle stream. In the absence of voltage, no detectable leakage through the microcapillaries could be found as the pressure-driven flow rates in the respective channels were initially balanced such that neither stream displaces the other. This oscillating field driven injection of liquids is believed to be an outcome of Maxwell-Wagner polarization as further discussed below.^{12,13}

To evaluate the characteristics of forces involved, the average velocity of particles pulled in the direction perpendicular to their flow was measured, while varying the applied voltage, for 10 μm particles at 4 distinct immersion conductivity levels (10, 25, 50, and 100 $\mu\text{S/cm}$). This involved measuring the displacement of the particles as a function of time from each frame of the movies recorded by a high-speed camera. Fig. 3 shows the measurements in plots where the average velocity, $|\bar{v}_p|$, can be seen as a nonlinear function of the applied voltage rms magnitude, V , and with almost no dependence on the frequency of the voltage applied over a range of values from 0.5 to 500 kHz. Describing the relation simply as $|\bar{v}_p| = k_1 V^2 + k_2 V$, where k_1 and k_2 the least-square fitting parameters, $R^2 > 0.94$, one could associate the quadratic term with DEP and the linear term with EP as the two possible scenarios. Few pending points cast doubt on the either situation. First, the particles with immersion conductivity levels in excess of 1 $\mu\text{S/cm}$ were always found repelled by the microcapillary openings, regardless of the field frequency applied, when the voltage was delivered through liquid metal filling the microcapillaries. Second, EP typically requires a non-oscillating field and must vanish for the field oscillations here. In Fig. 3(a), the solid lines represent the least-square fits to the data rather according to $|\bar{v}_p| = k_1 V^3 + k_2 V$, with the fitting values as listed in supplementary material (Table S-I, $R^2 > 0.96$).¹⁵ In the remaining, we argue that the cubic term arises from the CP force whereas the linear term can be attributed to DP, i.e., $\bar{v}_p = \bar{v}_{CP} + \bar{v}_{DP}$.

When an electrolyte with a concentration gradient is subjected to an electric field, free charges are generated to preserve electrical current against slight deviations from electroneutrality brought by the electromigration of ions. In an analogy to the hydrostatic pressure exerted by gravity, this leads to a pressure field (p_s) in liquid with Coulombic force acting on the free charges, i.e., $\nabla p_s = \rho_f \bar{E}$ where ρ_f is the free charge density and \bar{E} is the electric field vector with a strength depending on the local concentration.⁸ Since the electrical pressure is inversely proportional to the

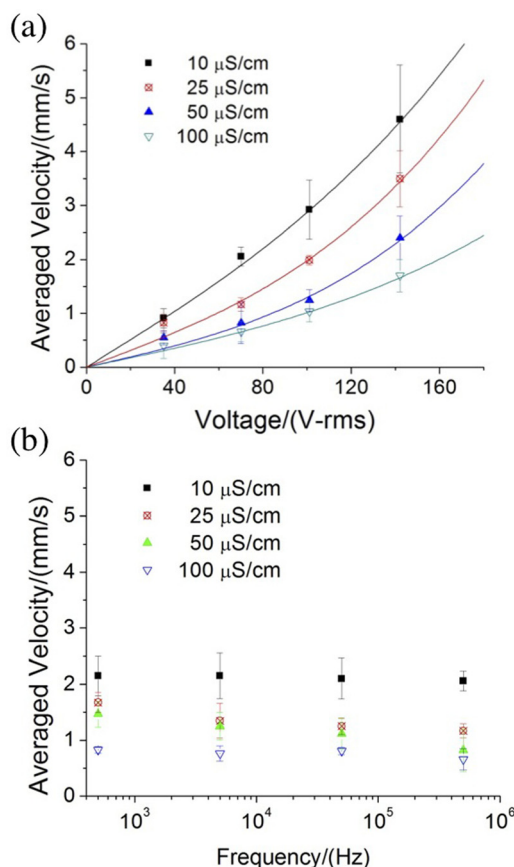


FIG. 3. Measured average trapping velocity of 10 μm particles pulled in the direction perpendicular to their flow in the center channel as a function of the externally applied voltage oscillation (a) rms magnitude and (b) frequency for a set of distinct immersion conductivity values (legend). The conductivity of the electrolyte in the outer channels was 15 mS/cm. The streams were maintained under pressure-driven flow at a rate of 0.68 $\mu\text{l/min}$ in the outer channels and 0.17 $\mu\text{l/min}$ in the center channel (from right to left). The microcapillaries were at a nominal width and depth of 2 μm . The symbols and error bars indicate the experimentally measured mean \pm s.d. ($n = 5$). The solid lines are the least-square fits to the data: (a) 500 kHz and (b) 71 V-rms.

concentration (conductivity), a dielectric particle immersed in such liquid would experience higher pressure on the low conductivity side than on the high conductivity side and be pushed accordingly up the concentration gradient, $\nabla(c)$. This leads to a pressure force on the particle and, along with the dielectrophoretic force due to the nonuniform electric field (DEP) and the hydrodynamic force due to the nonuniform pressure field, constitutes the CP force (\bar{F}_{CP}). Kang and Li, through a detailed perturbation analysis, derived the following:

$$\bar{F}_{CP} \approx 3.46\pi a^3 \epsilon_r \epsilon_0 E_0^2 \nabla \log(c), \quad (1)$$

where a is the particle radius, ϵ_r is the relative permittivity of water, $\epsilon_0 = 8.85 \times 10^{-12}$ F/m is the vacuum dielectric constant, E_0 is the electric field magnitude, and c is the ionic concentration. Although the derivation of Eq. (1) is based on a non-oscillating field, it is expected that the CP force persist in oscillating fields, since the polarity of free charges generated will be reversed with the field cycle. Hence, the CP force is always directed towards the region of higher concentration, irrespective of the direction of the applied voltage.

This is in agreement with our experimental observations; the particles are pulled towards the microcapillary openings as long as the pulling force is not strongly opposed by the oscillating field-driven injection of electrolytes invading the particle stream (further on this, below).

The CP force on the particles is balanced by the Stokes drag force, which can be stated as $\vec{F}_S = 6\pi\eta a\vec{v}_{CP}$, neglecting the velocity component of the flow due to the oscillating field-driven injection of electrolytes to the particle stream. The particle velocity due to the CP force can then be expressed as

$$\vec{v}_{CP} \approx 0.58 \frac{\epsilon_r \epsilon_0}{\eta} (\lambda Va)^2 \nabla \log(c), \quad (2)$$

where η is the viscosity, and λ is a geometric factor introduced to relate the electric field to the applied voltage rms magnitude. Equation (2), although it implicates a quadratic relation to the applied voltage, can be utilized to model the cubic term ($k_1 V^3$). This is because in our configuration the $\nabla \log(c)$ depends on the applied voltage. In the absence of an applied voltage, concentration (conductivity) gradient in the device arises from diffusion of ions as the flow rates were initially balanced to minimize convection through the microcapillaries. However, as soon as the voltage oscillation was turned on, electrolytes were observed to stream out and displace the center flow. This is evident in the images presented in Fig. 2. Moreover, the center flow at the downstream of the microcapillaries exhibited proportionally increased fluorescence intensity with the applied voltage rms magnitude and the particle immersion conductivity level in relation to that of the electrolyte. This correlation may not be that obvious in the presented high-speed video microscopy stills, which were taken under a limited exposure time.

The observed injection of the electrolyte might stem from electrothermal effects where Joule heating gives rise to spatial variations in electrical properties of the liquids near the microcapillaries and the subsequent generation of free volume charge upon which Coulomb forces act.¹⁴ However, this is less likely to occur as the heat generated will be readily removed in a convective flow-through system. Moreover, our simulations indicate only a few degrees rise above room temperature. It is more likely that the electrolyte injection is a consequence of the electrical interface between the electrolyte and the particle immersion. Such interface is expected to undergo a conductivity-dependent Maxwell-Wagner polarization with the applied voltage.^{13,14} Free charges are induced at the interface due to the jump in the normal component of the displacement vector. The induced charges switch sign with the reversal of the voltage polarity, rendering the interface susceptible to a nonzero time-averaged electrical force towards the less conducting particle stream.

The $\nabla \log(c)$ can be further related to the applied voltage in our device through diffusiophoresis,⁷ which is the motion of particles induced by a solute concentration gradient and could explain the linear dependence on the rms voltage ($k_2 V$). For a binary electrolyte such as *NaCl*, the main constituent of the PBS composition here, the diffusiophoretic velocity of a particle is given by

$$\vec{v}_{DP} = D_{DP} \nabla \log(c), \quad (3)$$

where D_{DP} is the diffusiophoretic mobility which has the same unit as diffusion coefficient and calculated as

$$D_{DP} = \frac{k_B T}{\eta} \frac{[-\log(1 - \gamma^2) + (1/2)\beta\Psi]}{2\pi\ell_B}, \quad (4)$$

where $\beta = D^+ - D^- / D^+ + D^-$ is the ion specific factor, $\Psi = z_0 e \zeta / k_B T$ is the normalized zeta potential, $\gamma = \tanh(\Psi/4)$ and $\ell_B = (z_0 e)^2 / 4\pi\epsilon_r \epsilon_0 k_B T$ is the Bjerrum length (D^\pm and z_0 the diffusion coefficients and the valence of the ions, respectively, ζ the zeta potential of the particles and e , k_B , and T , respectively, the elementary charge, the Boltzmann constant and absolute temperature such that the thermal potential at room temperature is $k_B T / e = 25$ mV). We assume that $D^+ = 1.4 \times 10^{-9}$ m²/s for Na⁺ and $D^- = 2.0 \times 10^{-9}$ m²/s for Cl⁻; hence, $\beta = -0.176$.

To validate our argument, we numerically evaluated particle trajectories in a 3D model and compared them against the experimentally obtained trajectories. Specifically, we considered the particle motion under the combined influence of the CP force, diffusiophoresis, and Stokes drag, $\vec{F}_{CP} + \vec{F}_{DP} + \vec{F}_S = m_p \dot{\vec{v}}_{CP}$, where the dot denotes time derivative of \vec{v}_{CP} and $m_p = 3\pi a^3 \rho_p / 4$ is the mass of the spherical polystyrene particle with radius $a = 10$ μ m and mass density $\rho_p = 1060$ kg/m³. The instantaneous position of the particle \vec{x}_p was then computed by integrating the particle velocity over time. Equation (1) was used for the CP force whereas the DP force was balanced by the viscous drag due to the velocity term \vec{v}_{DP} given by Eq. (3), i.e., $\vec{F}_{DP} = 6\pi\eta a D_{DP} \nabla \log(c)$. Stokes drag was assumed to be $\vec{F}_S = 6\pi\eta a (\vec{v}_f - \vec{v}_p)$, with \vec{v}_f being the local velocity of the fluid. The required distributions of electric, concentration and hydrodynamic fields were obtained by simultaneously solving the Poisson–Nernst–Planck and the Stokes (PNP–S) equations for the 3D geometry. The liquid conductivity levels were set at the stated values and the electrical boundary condition was defined at 71 V-rms, 500 kHz. Note that any perturbation to the field distribution caused by the presence of the particle was neglected. Further details of the computational model including the boundary conditions, material properties, and the key simulation results are as presented in supplementary material.¹⁵

The simulated trajectories of 10- μ m particles were compared against the trajectories experimentally obtained under the conditions similar to the ones used in the simulations and found in good qualitative agreement (Fig. 4). More importantly, the simulations predict the trapping events of the particles at the microcapillary openings. The CP force and the force due to diffusiophoresis amount to a total trapping force of ~ 1 nN, when averaged along the representative trapping trajectory of the particle (200 simulated data points, supplementary material).¹⁵ From each simulated trajectory, the average velocity of the particle in the direction perpendicular to the flow was derived and compared against the experimentally measured value for the corresponding immersion conductivity level (Table I). Table I also lists the calculated and measured values of D_{DP} and ζ , respectively. The measured

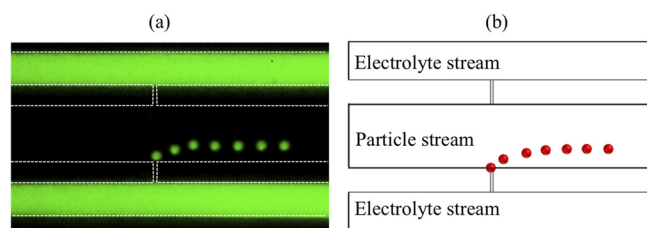


FIG. 4. Experimental and simulated trajectories of a 10- μm particle compared under excitation 71 V-rms, 500 kHz. The particle stream and the electrolyte streams were pressure-driven from right to left at a rate of 0.17 $\mu\text{l}/\text{min}$ and 0.68 $\mu\text{l}/\text{min}$, respectively. The streams were applied at a respective conductivity of 50 $\mu\text{S}/\text{cm}$ and 15 mS/cm. Overlays of high-speed video microscopy stills were taken at 4000 fps. The nominal width and depth of the microcapillaries were 2 μm . The dashed lines outline the channel and microcapillary boundaries.

TABLE I. The measured and predicted trapping velocity of 10- μm particles for the set immersion conductivity levels and the excitation at 71V-rms, 500 kHz. The corresponding values of ζ and D_{DP} are as listed.

c ($\mu\text{S}/\text{cm}$)	ζ (mV)	$D_{DP} \times 10^{10}$ (mm^2/s)	$ \bar{v}_p $ (mm/s)	
			Experiment	Simulation
10	-55.7 ± 4.7	3.02	2.06	3.21
25	-53.3 ± 4.1	2.81	1.24	1.62
50	-47.4 ± 3.6	2.39	0.82	1.03
100	-38.1 ± 2.7	1.80	0.66	0.84

trapping velocity was found to increase from 0.66 to 2.06 mm/s as the immersion conductivity was reduced from 100 to 10 $\mu\text{S}/\text{cm}$, whereas the respective simulations returned comparable values from 0.84 to 3.21 mm/s, signifying a discrepancy of <1.6 fold. Such reasonable agreement obtained is despite the simplifying assumptions and attests our argument that the particle motion can be adequately described by the CP force and diffusiophoresis.

The simulations also offer insight into the conductivity profile across the device. The simulated results concur with the assumption that the $\nabla \log(c)$ around the microcapillary opening varies linearly with the applied voltage rms magnitude. Moreover, the simulations predict the observed injection of the electrolyte into the particle stream with the applied potential.¹⁵ Lastly, one might argue that the particle trapping observed with the electrolyte is in accordance with nDEP. This could be on the basis of that the electrolyte injection into the particle stream with the applied voltage oscillations possibly alters the electric field distribution and creates a field minimum near the microcapillary openings. However, the simulations suggest otherwise; the field strength continues to rise toward the microcapillary opening despite the

increased conductivity due to the predominant corner effect.¹⁵ Nevertheless, DEP does occur in our platform due to the nonuniform electric field distribution and is already incorporated in the derivation of Eq. (1), the CP force. However, the EHD contribution of the CP force due to induced “free” charges dominates over the DEP force and thus causes the net force to be exerted on the particle towards the region of higher conductivity, which agrees well with our experimental observations.⁸

In conclusion, dielectric particle trajectories in the co-presence of a conductivity gradient and oscillating electric field gradient have been investigated by utilizing a flow-through microfluidic design. For the applied range of field frequencies, the trajectories have shown drastic deviation from those when the conductivity gradient is absent within the same design (liquid metal replacing the electrolyte). The results in the former case are attributed to the concentration polarization and diffusiophoretic forces acting on the particles, as opposed to the dielectrophoretic force in the latter. Particle trajectories have been simulated based on the analytical expressions of such forces and the field distributions obtained from solving PNP-S equations for a 3D computational model. The simulated and experimentally observed trajectories have shown qualitative agreement, predicting the particle trapping at the microcapillary openings in the dilute immersion range (<100 $\mu\text{S}/\text{cm}$).

This research was supported by a grant from the Research Grant Council of Hong Kong (No. GRF621711).

¹B. Kirby, *Micro-And Nanoscale Fluid Mechanics: Transport in Microfluidic Devices* (Cambridge University Press, Cambridge, 2010).

²A. Ajdari, *Phys. Rev. Lett.* **75**, 755 (1995).

³D. J. Harrison, A. Manz, Z. Fan, H. Luedi, and H. M. Widmer, *Anal. Chem.* **64**, 1926 (1992).

⁴S. K. Cho, H. Moon, and C. J. Kim, *J. Microelectromech. Syst.* **12**, 70 (2003).

⁵P. R. Gascoyne and J. Vykoukal, *Electrophoresis* **23**, 1973 (2002).

⁶M. Z. Bazant and T. M. Squires, *Phys. Rev. Lett.* **92**, 066101 (2004).

⁷B. Abécassis, C. Cottin-Bizonne, C. Ybert, A. Ajdari, and L. Bocquet, *Nat. Mater.* **7**, 785 (2008).

⁸K. H. Kang and D. Q. Li, *J. Colloid Interface Sci.* **286**, 792 (2005).

⁹G. Goet, T. Baier, and S. Hardt, *Biomicrofluidics* **5**, 014109 (2011).

¹⁰R. Tornay, T. Braschler, and P. Renaud, *Lab Chip* **9**, 657 (2009).

¹¹Y. Luo, X. Cao, P. Huang, and L. Yobas, *Lab Chip* **12**, 4085 (2012).

¹²M. Desmond, N. Mavrogianis, and Z. Gagnon, *Phys. Rev. Lett.* **109**, 187602 (2012).

¹³P. Garcia-Sanchez, M. Ferney, Y. K. Ren, and A. Ramos, *Microfluid. Nanofluid.* **13**, 441 (2012).

¹⁴A. Castellanos, A. Ramos, A. Gonzalez, N. G. Green, and H. Morgan, *J. Phys. D: Appl. Phys.* **36**, 2584 (2003).

¹⁵See supplementary material at <http://dx.doi.org/10.1063/1.4894731> for detailed simulation methods and results.